Journal of Materials Science: Materials in Electronics
https://doi.org/10.1007/s10854-018-9320-9

Synthesis, characterization, magnetic and microwave absorption properties of iron–cobalt nanoparticles and iron–cobalt @ polyaniline (FeCo@PANI) nanocomposites

Mehdi Rahimi-Nasrabadi[1,2] · Mohammad Hosein Mokarian[3] · Mohammad Reza Ganjali[4,5] · Mohammad Almaci Kashi[6] · Sima Alikhanzadeh Arani[6]

Received: 13 March 2018 / Accepted: 17 May 2018

Abstract
In this research, iron–cobalt nanoparticles and iron–cobalt@polyaniline (FeCo@PANI) nanocomposite was prepared using two-step process including polyol process and in situ chemical oxidative polymerization. X-ray diffraction confirms the formation of FeCo alloy. As seen in VSM results FeCo@PANI nanocomposite leading to lower saturation magnetization and higher natural-resonance frequency than FeCo alloy. The effect of various parameters including solvent type, NaOH amount, sugar amount, sugar type, Fe/Co ratio and precursor type on the magnetic properties of prepared FeCo alloy have been investigated in details. The electromagnetic absorption characteristics of nanoparticle and nanocomposite were determined in the frequency range of 8–18 GHz. Results show that the PANI improves electromagnetic wave absorption properties of FeCo nanoparticles. The main mechanism enhancing the dielectric loss tangent is Deby's dual relaxation phenomenon and for magnetic loss is the ferromagnetic resonance. The maximum reflection loss of − 5.48 dB was obtained for 40 wt% FeCo@PANI nanocomposite with an effective absorption band (RL < − 3 dB) of 1.22 GHz.

1 Introduction

Nowadays, research on fabrication of nanosized materials has become a very interesting field in materials science. Materials with nanoscale dimensions usually show very different and interesting optical, magnetic, electronic, physical and chemical properties in comparison with those of their bulk materials [1–10].

Magnetic materials have gained a lot of attention in terms of both scientific and practical aspects. Among the various compounds with magnetic properties cobalt and iron are special due to their superior magnetic properties [11–13]. In many cases cobalt was added to other compounds to improve their coercivity. For example, coercivity of iron greatly increases by adding cobalt to iron in Fe–Co alloy. Furthermore Fe–Co alloy exhibit the highest saturation magnetization between the magnetic compounds. In addition, it shows high Curie temperature (~ 900 °C) and good permeability and mechanical properties. Because of these features Fe–Co alloy is one of the soft magnetic materials with wide range of applications, including electrical generators, transformer cores, microelectrochemical systems, microwave absorbing materials and protective coatings [14–18].

Nowadays, the fast development of the wireless communications has made electromagnetic wave absorption materials more attractive and various types of electromagnetic wave absorbers have been developed. Recently, considerable attentions have been paid to the development of high-efficient electromagnetic wave absorbers with strong absorption characteristics, wide absorption frequency,

✉ Mehdi Rahimi-Nasrabadi
rahimi@bmsu.ac.ir; rahiminasrabadi@gmail.com

1 Chemical Injuries Research Center, Baqiyatallah University of Medical Sciences, Tehran, Iran

2 Faculty of Pharmacy, Baqiyatallah University of Medical Sciences, Tehran, Iran

3 Department of Chemistry, Imam Hossein University, Tehran, Iran

4 Faculty of Chemistry, Center of Excellence in Electrochemistry, University of Tehran, Tehran, Iran

5 Biosensor Research Center, Endocrinology and Metabolism Molecular-Cellular Sciences Institute, Tehran University of Medical Sciences, Tehran, Iran

6 Institute of Nanoscience and Nanotechnology, Kashan University, Kashan, Iran

Published online: 11 June 2018

lightweight and good thermal stability [19–23]. Soft ferromagnetic nanoparticles like (e.g. FeCo) are good candidates for this purpose due to their high saturation magnetization, higher snoek's limit and high permeability at frequencies in the gigahertz range [24–29]. Based on the electromagnetic complementary theory, apart from dielectric loss and magnetic loss, a proper impedance matching between dielectric loss and magnetic loss also determines the reflection and attenuation characteristics [30, 31].

Recently, the fabrication of inorganic/conducting polymer materials has attracted a lot of interest [32–35]. Among many conducting polymers, polyaniline (PANI) has been considered as a promising candidate for electromagnetic wave absorbers due to its high conductivity, low density, easy preparation and good environmental stability [36–39]. However, pure PANI has high complex permittivity and low complex permeability, resulting in a poor impedance matching.

In this work, a novel nanocomposites of iron–cobalt alloy @ polyaniline (FeCo@PANI) have been prepared and the electromagnetic wave absorption properties were investigated. As electromagnetic wave absorption materials, the nanocomposites exhibit excellent electromagnetic wave absorption properties and wide absorption bandwidths compared with FeCo nanoparticle. When the thickness is 3 mm, the maximum reflection loss (RL) of FeCo@PANI is − 5.48 dB at 9.4 GHz and the absorption bandwidths − 3 dB are 1.22 GHz.

2 Experimental

2.1 Materials and characterization

Fe(II) chloride tetrahydrate, Co(II) acetate tetrahydrate, propylene glycol (PG), sodium hydroxide (NaOH), aniline monomer (ANI), ammonium persulfate (APS), p-toluenesulfonic acid (p-TSA) were purchased from MERCK Company and used as received without further purification. The samples were examined at room temperature on an X-ray powder diffractometer (XRD) for phase identification using CuKα radiation. Sample morphology was studied using a field-emission scanning electron microscope (FE-SEM). The magnetic properties of samples were investigated at room temperature by a vibrating sample magnetometer (VSM, Meghnatis Kavir Kashan Co., Kashan, Iran). The RL of a composite sample which contained 25 wt% of FeCo/PANI composites (The content of powder in the epoxy resin matrix was 25 wt% for all the specimens) was measured using a vector network analyzer (VNA) in the frequency range of 8–18 GHz.

2.2 Preparation of FeCo nanoparticles

For the synthesis of FeCo nanoparticles, a one pot polyol procedure was designed. In a typical synthesis procedure, 100 mL of propylene glycol (PG) was heated in a reaction vessel up to a temperature of 170 °C. The total metal salts concentration was fixed at 0.1 mol/L and the Fe/Co molar ratio was varied according to the anticipated final alloy composition. The precursor salts, Fe(II) chloride tetrahydrate, and Co(II) acetate tetrahydrate were weighed, physically mixed thoroughly, and added to this solution. After 1 min, appropriate amount of NaOH pellets (1.6, 3.2 and 4.8 g) were added and the mixture was stirred at 300 rpm. Immediately, the solution starts bubbling, and the formation of alloy was indicated by the gray color of supernatant solution. The heater was then turned off and stirring was continued while the solution cooled slowly. The recovery of the particles from the solution is easier at a temperature slightly higher than room temperature due to the lower viscosity of the solvent. The solution was centrifuged, washed several times with methanol, and the black colored FeCo particles were magnetically separated and stored in methanol.

2.3 In situ preparation of FeCo@PANI nanocomposites

The FeCo@PANI nanocomposites were synthesized by an in situ chemical oxidative polymerization in the presence of FeCo with APS as oxidant and p-TSA as dopant. A typical preparation process was carried out as follows: p-TSA (0.0344 g) was dissolved in distilled water (30.0 mL), and then aniline (0.25 mL) and FeCo powders (0.2 g) were added to the above mixture. Then the mixture was uniformly homogenized with ultra-sonication for 60 min and 5 mL of APS (0.627 g) aqueous solution was slowly added into the mixed solution. Then the mixture was allowed to react for 4 h with vigorous mechanical stirring under ice-water bath. The final products were thoroughly washed with distilled water and methanol for several times, and finally dried at 60 °C for 24 h to obtain the dark powders of FeCo@PANI nanocomposites [40, 41].

3 Results and discussion

3.1 Synthesis of FeCo alloy and investigation of its properties

For the formation of FeCo alloy, co-reduction of Fe and Co has to be achieved which can be explained based on the following reactions [42–45]:

$$C_3H_8O2 \xrightarrow{\Delta} C_3H_5OH \quad (1)$$

$$2C_3H_5OH + FeCl_2 \xrightarrow{\text{Excess NaoH}} C_6H_{10}O_2 + 2H_2O + Fe^0 \quad (2)$$

$$C_3H_5OH + CoCl_2 \xrightarrow{\text{Excess NaoH}} C_3H_5O_2 + H_2O + Co^0 \quad (3)$$

In the above Eq. (2), the experimental condition must be controlled in such a way that Fe^{2+} ions directly reduces to Fe without forming $Fe(OH)_2$. The high concentration of OH^- ions enhances the continuous dehydration of polyol and formation of acetaldehyde by facilitating the electron transfer from polyol to the ionic species, thereby resulting in the reduction of Fe. In the case of Co as per Eq. (3), the reduction is preceded by the formation of alkoxide and dissolution. The presence of hydroxide ions accelerates the above reduction process. However, the presence of hydroxide ions is more critical for the reduction of Fe compared to Co since the standard reduction potential (SRP) of Fe is lower than the polyol reduction limit.

Figure 1 showed the powder X-ray diffraction pattern of the resultant product. The peaks could be assigned to the (110), (200), and (211) reflections of the cubic FeCo alloy (JCPDS No. 49-1568), respectively. No impurities such as $Co(OH)_2$, $Fe(OH)_2$, and oxides were detected, indicating that the obtained FeCo alloy was highly pure and the co-reduction of metal salts to alloy was complete. The crystallite size measurements were carried out using the Scherrer equation:

$$D_c = K\lambda/\beta\cos\theta$$

where β is the width at half maximum intensity of the observed diffraction peak, and λ is the X-ray wavelength (CuKα radiation, 0.154 nm). The estimated crystallite size is about 20 nm.

Field-emission Scanning electron microscope images of nanoparticles are illustrated in Fig. 2. As can be seen, nanoparticles with average diameter of about 30 nm were obtained. The room temperature magnetic properties of the FeCo and FeCo@PANI samples were studied with a vibrating sample magnetometer (VSM). Figure 3a shows the hysteresis loop of the FeCo sample with a saturation magnetization of 66 emu/g and coercivity of 380 Oe. The saturation magnetization is lower than that for the same bulk composition [46] which may be due to the presence of thin layer of oxide surface or the formation of amorphous phase with alloy phase. The oxide layer is present in most of the chemically synthesized FeCo samples [47]. As well, Fig. 3b shows the hysteresis loop of the FeCo@PANI sample were synthesized by an in situ chemical oxidative polymerization with a saturation magnetization of 1.17 emu/g and coercivity of 270 Oe. Reduce the amount of saturation magnetization is due to the low percentage of FeCo in nanocomposite.

3.1.1 Effect of solvent type on the magnetic properties of FeCo alloy

FeCo alloy nanoparticles have been synthesized in two different solvent system including ethylene glycol (EG) and propylene glycol (PG) and the magnetic properties of prepared NPs have been compared (Fig. 4). The results of Fig. 4 confirm that the saturation magnetization of two samples are in same order of about 132 emu/g, but the coercivity of prepared sample in EG in comparison to the PG sample reduced from 366 to 275 Oe.

3.1.2 Effect of NaOH amount on the magnetic properties of FeCo alloy

Figure 5 shows the effect of NaOH amount on the saturation magnetization and coercivity of prepared Fe–Co alloy nanoparticles. As shown in this figure the greatest saturation magnetization and coercivity is observed in sample prepared with 1.6 g of NaOH. The saturation magnetization and coercivity of this sample are 132 emu/g and 366 Oe, respectively.

3.1.3 Effect of sugar amount and sugar type on the magnetic properties of FeCo alloy

Selecting an appropriate reducing agent plays an important role to achieve high saturation magnetization. In the present study sucrose, glucose, maltose, and starch were studied as reducing agent.

Effects of sucrose amount on magnetic properties of alloy have been investigated in different precursor (Fe or Co) to sucrose ratio and the results of these experiments have been shown in Fig. 6 and Table 1. As can be seen from the results the highest magnetization is achieved with a ratio of 1.5, while the coercivity of samples is in relatively same order. Thus 1.5 has been chosen as optimum ratio and other sugar have been investigated with this ratio as optimum value.

In the next step of this study the effect of sugar type on magnetic properties of prepared samples have been investigated. The hysteresis loop of prepared samples with glucose, starch and maltose with the sugar to precursor ratio of 1.5 have been shown in Fig. 7 and the results are compared in Table 2. As can be seen from the results the highest magnetization is obtained by using sacarose as capping agent (186 emu/g) and the lowest value with maltose prepared sample (65 emu/g). Furthermore the highest coercivity was achieved with the sample prepared with sacarose (327 Oe) and the lowest coercivity with starch (220 Oe) prepared sample.

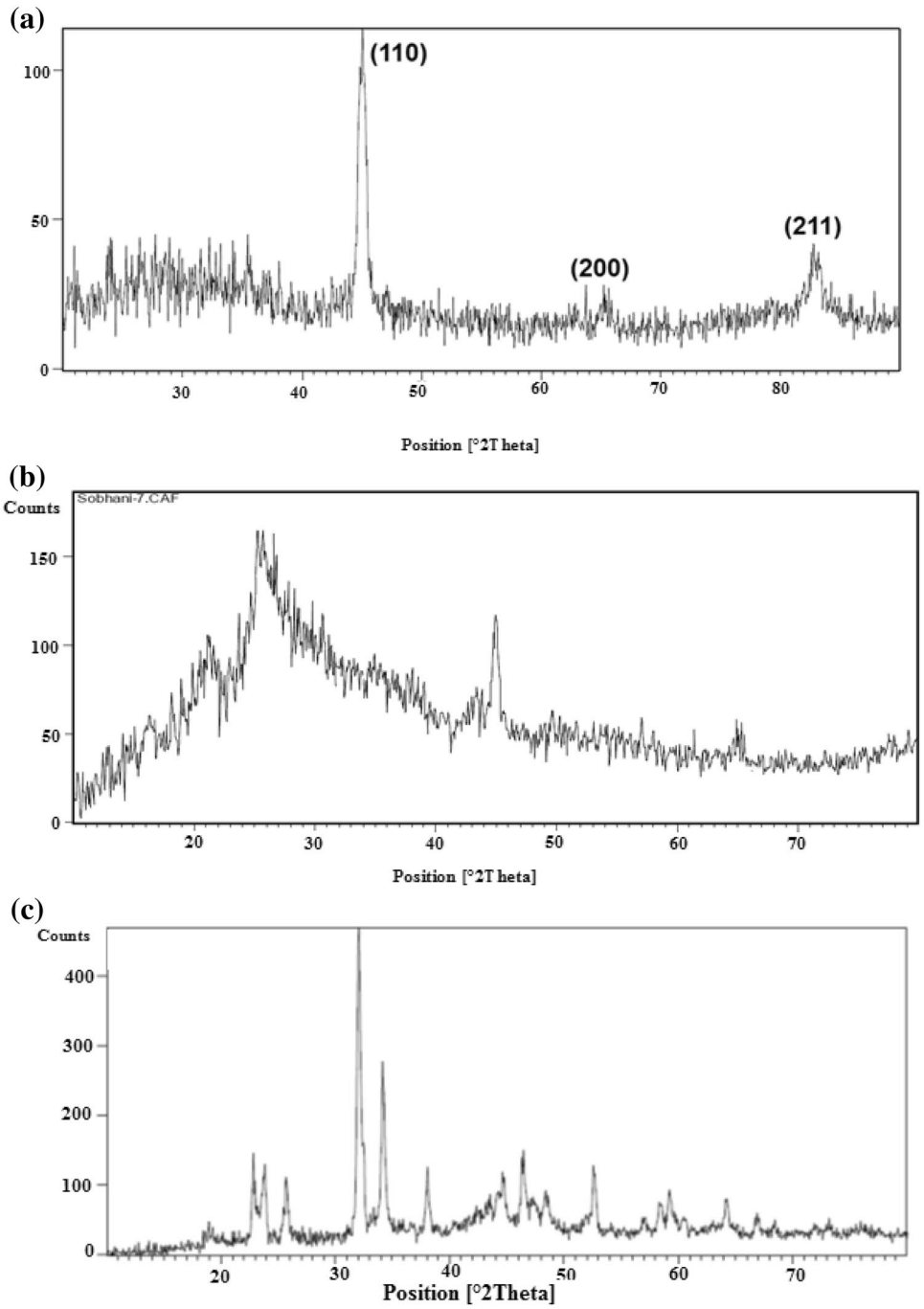

Fig. 1 XRD patterns of **a** FeCo nanoparticles and **b** FeCo@PANI nanocomposite

3.1.4 Effect of Fe/Co ratio on the magnetic properties of Fe:Co alloy

In order to investigate the effect of Fe:Co ratio on magnetic properties of prepared samples, some sample containing different ratio of Fe:Co have been prepared. The results of individual study have been shown in Figs. 8 and 9. As can be seen the highest saturation magnetization and coercivity was achieved with Fe:Co ratio of 70:30%. It was observed that the saturation magnetization was decreased with the increase of Fe amount from 30 to 50, and then increased by further enhancement of the Fe amount to 70. In the other hand the coercivity of sample will increase with increasing the amounts of Fe percent from 30 to 50 and 70.

3.1.5 Effect of precursor type on the magnetic properties of FeCo alloy

In order to explore the effect of precursor type on the magnetic properties of prepared sample different precursor have

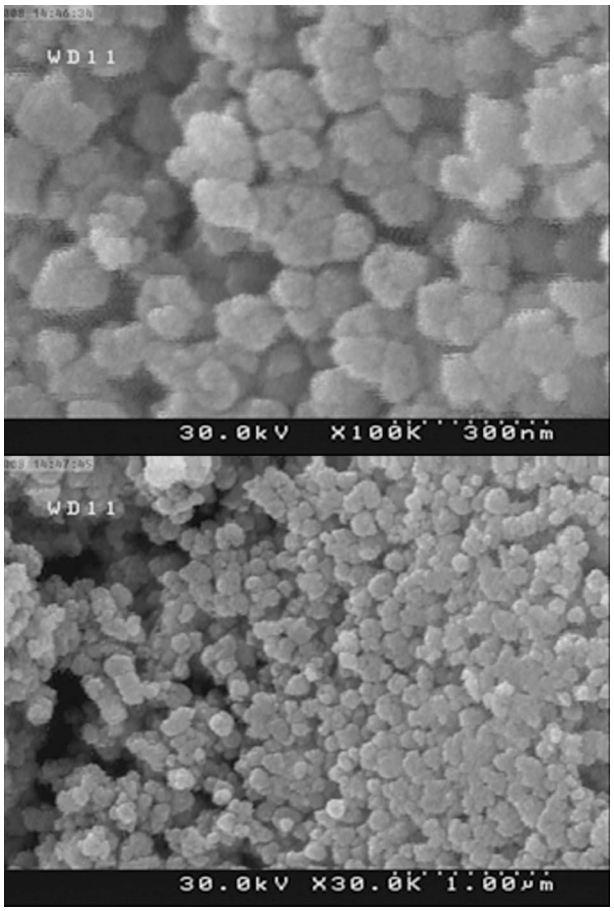

Fig. 2 SEM of FeCo nanoparticle synthesized using a polyol process

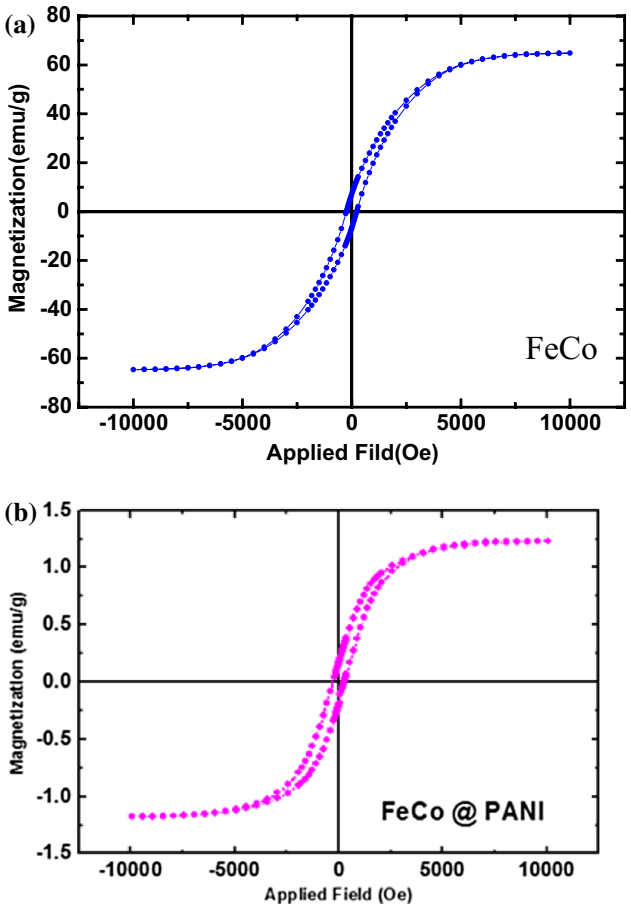

Fig. 3 Magnetization hysteresis loops of **a** FeCo nanoparticles and **b** FeCo@PANI nanocomposite measured at room temperature

been tested. Among various precursor (sulfate, nitrate, chloride and acetate) two precursor including chloride and acetate lead to the production of FeCo alloy. Using precursor like ferric sulfate and cobalt sulfate the FeCo alloy was not formed. The XRD pattern of sample prepared with sulfate precursor was shown in Fig. 1c. As can be seen from this figure the XRD pattern is not match with the pattern of FeCo alloy. On the other hand the hysteresis loop of this sample have been shown in Fig. 10, the saturation magnetization value of this sample is very lower than expected value for FeCo alloy.

The hysteresis loop of Fe/Co sample prepared with $FeCl_2/CoCl_2$ and $FeCl_2/Co(CH_3COO)_2$ precursor compared if Fig. 11. As can be seen the prepared sample with chloride precursor (a) have higher saturation magnetization and lower coercivity compared to produced sample with acetate precursor.

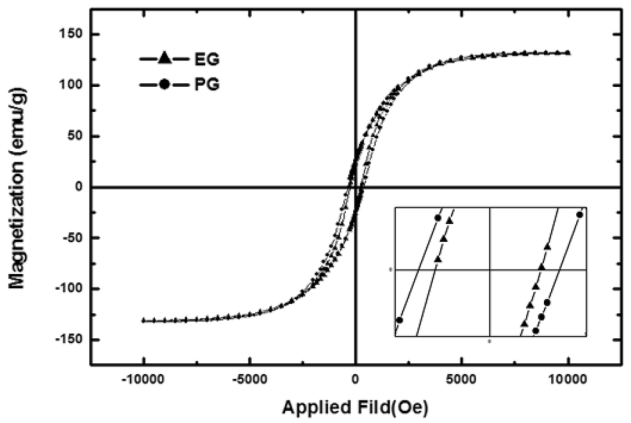

Fig. 4 Effect of solvent type on the hysteresis loop of Fe/Co alloy in the presence of EG and PG as solvent

3.2 Microwave absorbing properties

In order to compare the electromagnetic wave absorption behavior of Fe/Co nanoparticles with CoFe/PANi nanocomposites, the RL of CoFe/PANi is calculated according to transmission line theory as follows [48]:

$$\mathrm{RL(dB)} = 20\log\left|\frac{Z_{in}-1}{Z_{in}+1}\right|$$

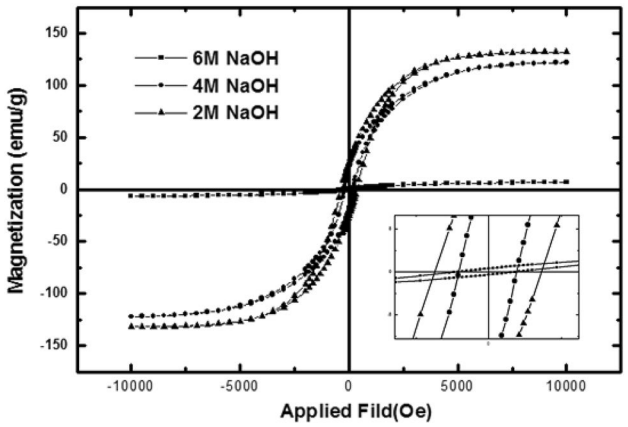

Fig. 5 Effect of NaOH amount on the hysteresis loop of Fe/Co alloy

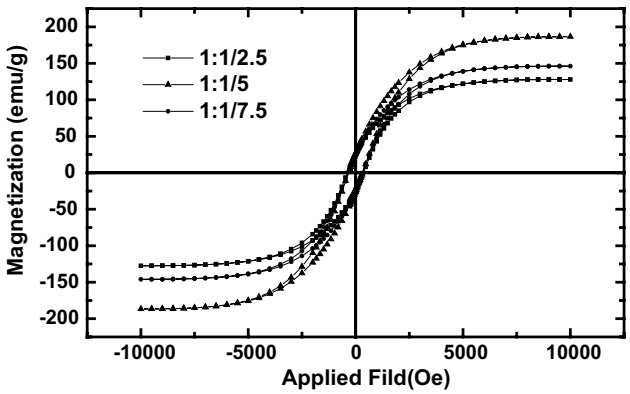

Fig. 6 Effect of sucrose amount on the hysteresis loop of Fe/Co alloy at different precursor (Fe or Co) to sucrose ratio

Table 1 Effect of sucrose amount on the magnetic properties of Fe/Co alloy

Precursor/sucrose ratio	M_s (emu/g)	H_c (Oe)
1/1.25	127	358
1/1.5	186	327
1/1.75	146	308

$$Z_{in} = \sqrt{\frac{\mu_r}{\varepsilon_r}} \tanh\left[j\left(\frac{2\pi fd}{c}\right)\sqrt{\varepsilon_r \mu_r}\right]$$

where Z_{in} is the input impedance of the absorber, c is the velocity of light in free space, f is the frequency and d is the layer thickness. Thus, the RL values of the absorbers with filler loadings of 40 vol% at various thicknesses can be obtained, as shown in Fig. 12. The effect of PANI on the electromagnetic wave absorption properties is clearly seen from the figure. For FeCo nanoparticles (Figs. 12a) the maximum RL of − 3 dB at 15.9 GHz has been obtained

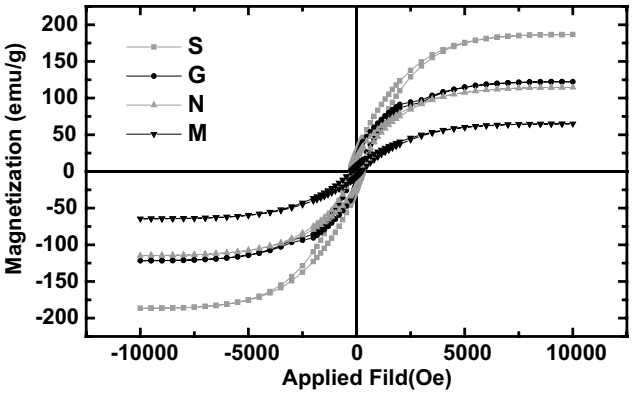

Fig. 7 Comparison of hysteresis loop of various Fe/Co alloy prepared with different sugar

Table 2 Effect of sugar type on the magnetic properties of Fe/Co alloy

Sugar type[a]	M_s (emu/g)	H_c (Oe)
Sucrose	186	327
Glucose	122	302
Starch	114	220
Maltose	65	240

[a]The precursor to sugar ratio is 1.5 for all sugar

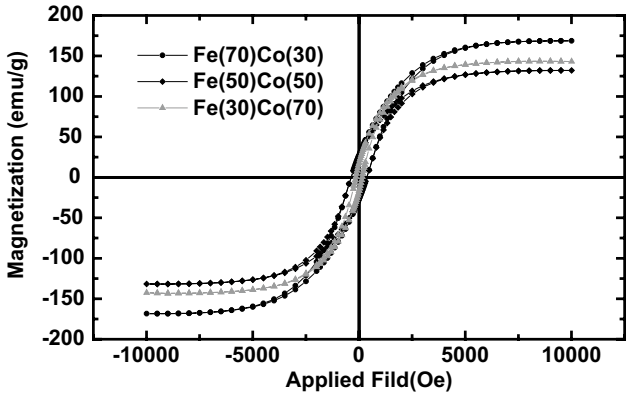

Fig. 8 Effect of Fe/Co ratio on the magnetic properties of Fe/Co alloy

for 3 mm thickness. But for FeCo@PANI nanocomposite (Fig. 12b) maximum RL of − 5.48 dB (equivalent to 71% of the absorption of waves) at 9.4 GHz has been obtained for 3 mm thickness. Also the optimal RL and effective bandwidths for FeCo@PANI nanocomposite are brought to Table 3. As seen from the data presented in Table 3 the bandwidth in which 50% of the incident wave is absorbed (RL < − 3 dB) is maximum for 3 mm (1.22 GHz) thickness which also has the maximum RL of − 5.48 dB.

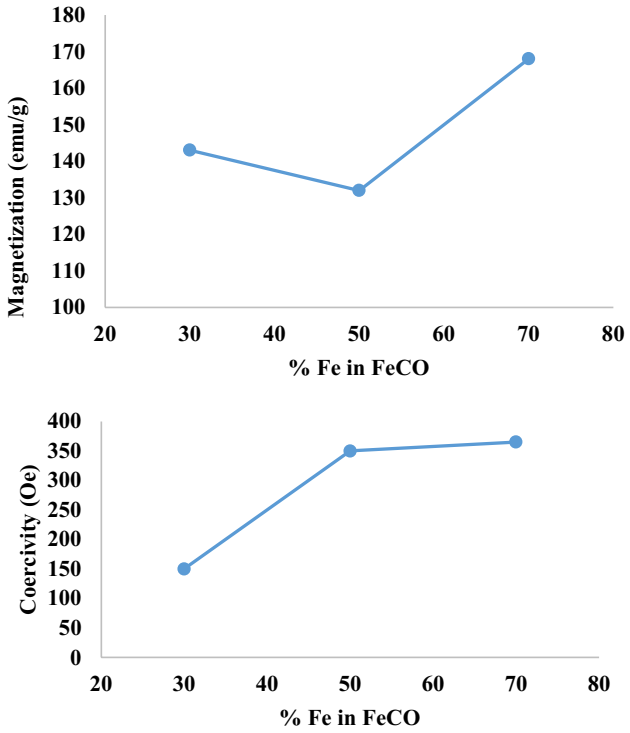

Fig. 9 Effect of Fe amount on the saturation magnetization and coercivity of Fe/Co alloy

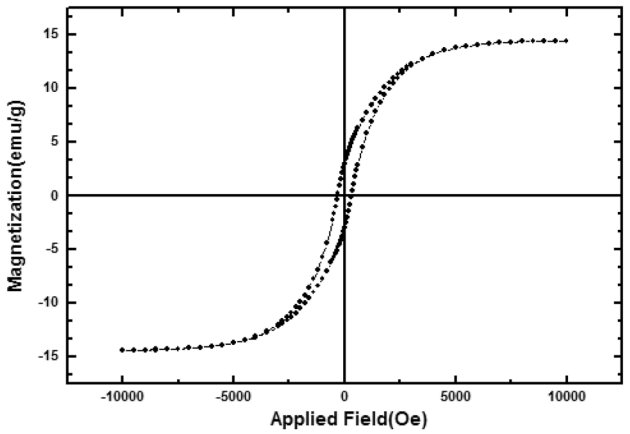

Fig. 10 Hysteresis loop of sample prepared with $FeSO_4$ and $CoSO_4$ as precursor

Furthermore, as seen from Fig. 11, by reducing the thickness of both sample, the yield is reduced. As a result, the electromagnetic wave absorption properties and the absorption bandwidths of the nanocomposites are better than the pure nanoparticles, thus, the nanocomposites with excellent electromagnetic wave absorption properties can be used as lightweight electromagnetic wave absorbing materials.

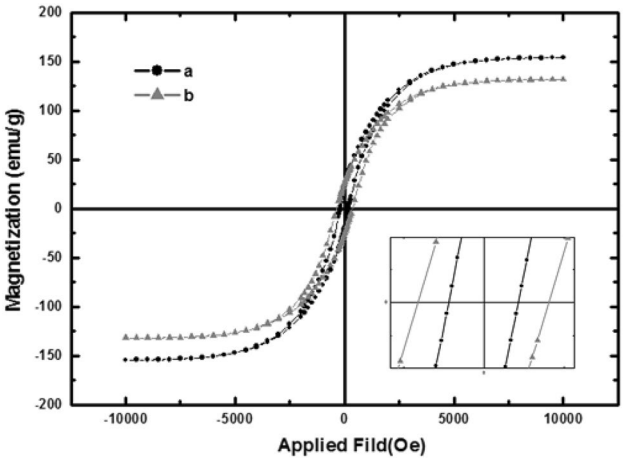

Fig. 11 Effect of precursor type on the magnetic properties of Fe/Co alloy. **a** Prepared by $FeCl_2$ and $CoCl_2$, **b** prepared by $FeCl_2$ and cobalt acetate

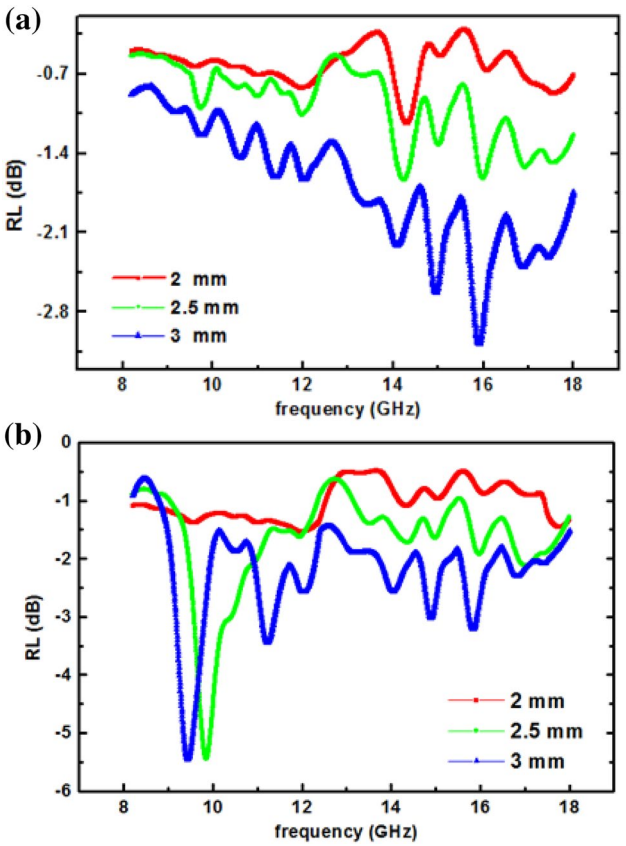

Fig. 12 Frequency dependence of RL for nanocomposite containing 40 vol%. **a** FeCo nanoparticles, **b** FeCo@PANI nanocomposite at various thicknesses

Table 3 Microwave absorbing properties of Fe–Co nanoparticles and FeCo@PANI nanocomposites

Sample	Layer thickness (mm)	Maximum RL (dB)	Equivalent to the maximum RL (%)	Maximum RL frequency (GHz)	Bandwidth equivalent to the 50% (RL < − 3 dB) (GHz)
FeCo@PANI	3	− 5.48	71.68	9.4	1.22
FeCo@PANI	2.5	− 5.43	71.35	9.86	0.86
FeCo	3	− 3	50	15.9	0

4 Conclusion

FeCo nanoparticles were synthesized using a polyol process. Then FeCo@PANI nanocomposite was synthesized by an in situ chemical oxidative polymerization in the presence of FeCo. The effect of PANI on the magnetic properties of FeCo nanoparticles was investigated. VSM results of FeCo@PANI nanocomposite show lower saturation magnetization (1.17 emu/g) compared with that of FeCo nanoparticles (66 emu/g). This is due to the non-magnetic PANI of FeCo nanocomposite which decreases the saturation magnetization. Incorporation of the PANI into FeCo nanoparticle improves the microwave absorption properties of FeCo@PANI nanocomposite due to activation of several dielectric-magnetic loss mechanisms including dual dielectric relaxation and magnetic ferromagnetic resonance. The maximum RL of − 5.48 dB was obtained for 40 vol% FeCo@PANI nanocomposite with an effective absorption band (RL < − 3 dB) of 1.22 GHz.

Acknowledgements The financial support of this work by Baqiyatallah University of Medical Sciences is gratefully acknowledgments.

References

1. M. Mousavi, A. Habibi-Yangjeh, J. Mater. Sci. Mater. Electron. **27**, 8532 (2016)
2. M. Salavati-Niasari, F. Soofivand, A. Sobhani-Nasab, M. Shakouri-Arani, M. Hamadanian, S. Bagheri, J. Mater. Sci. Mater. Electron. **28**, 14965 (2017)
3. S. Ramezani, A. Ghazitabar, S.K. Sadrnezhaad, J. Iran. Chem. Soc. **13**, 2069 (2016)
4. S. Pourmasoud, A. Sobhani-Nasab, M. Behpour, M. Rahimi-Nasrabadi, F. Ahmadi, J. Mol. Struct. **1157**, 607 (2018)
5. S.M. Pourmortazavi, S.S. Hajimirsadeghi, M. Rahimi-Nasrabadi, Mater. Sci. Semicond. Process. **16**, 131 (2013)
6. S.M. Pourmortazavi, S.S. Hajimirsadeghi, M. Rahimi-Nasrabadi, I. Kohsari, Synth. React. Inorgan. Met. Organ. Nano Met. Chem. **42**, 746 (2012)
7. M. Rahimi-Nasrabadi, F. Ahmadi, M. Eghbali-Arani, J. Mater. Sci. Mater. Electron. **27**, 11873 (2016)
8. S.S. Hosseinpour-Mashkani, A. Sobhani-Nasab, J. Mater. Sci. Mater. Electron. **28**, 16459 (2017)
9. M. Shamsipur, S.M. Pourmortazavi, S.S. Hajimirsadeghi, M.M. Zahedi, M. Rahimi-Nasrabadi, Ceram. Int. **39**, 819 (2013)
10. M. Rahimi-Nasrabadi, S.M. Pourmortazavi, M.R. Ganjali, A.R. Banan, F. Ahmadi, J. Mol. Struct. **1074**, 85 (2014)
11. M. Rahimi-Nasrabadi, M. Behpour, A. Sobhani-Nasab, S. Mostafa Hosseinpour-Mashkani, J. Mater. Sci. Mater. Electron. **26**, 9776 (2015)
12. M. Rahimi-Nasrabadi, M. Rostami, F. Ahmadi, A. Fallah Shojaie, M. Delavar Rafiee, J. Mater. Sci. Mater. Electron. **27**, 11940 (2016)
13. M. Rahimi-Nasrabadi, M. Behpour, A. Sobhani-Nasab, M. Rangraz Jeddy, J. Mater. Sci. Mater. Electron. **27**, 11691 (2016)
14. N.M. Nik Rozlina, A.M. Alfantazi, Mater. Sci. Eng. A **550**, 388 (2012)
15. I. Tabakovic, S. Riemer, N. Jayaraju, V. Venkatasamy, J. Gong, Electrochim. Acta **58**, 25 (2011)
16. S.K. Pal, D. Bahadur, Mater. Lett. **64**, 1127 (2010)
17. S. Costacurta, L. Malfatti, P. Innocenzi, H. Amenitsch, A. Masili, A. Corrias, Microporous Mesoporous Mater. **115**, 338 (2008)
18. Q. Wang, S. Li, W. Xu, Y. Chen, H. Yang, J. Mater. Sci. Mater. Electron. **20**, 1172 (2009)
19. B. Lu, X.L. Dong, H. Huang, X.F. Zhang, X.G. Zh, J.P. Lei, J.P. Sun, J. Magn. Magn. Mater. **320**, 1106 (2008)
20. X. Liu, S.W. Or, S.L. Ho, C.C. Cheung, C.M. Leung, Z. Han, D. Geng, Z. Zhang, J. Alloys Compd. **509**, 9071 (2011)
21. B. Wang, J. Zhang, T. Wang, L. Qiao, F. Li, J. Alloys Compd. **567**, 21 (2013)
22. D. Hasegawa, H. Yang, T. Ogawa, M. Takahashi, J. Magn. Magn. Mater. **321**, 746 (2009)
23. H.T. Yang, D. Hasegawa, M. Takahashi, T. Ogawa, Appl. Phys. Lett. **94**, 013103 (2009)
24. S. Yan, L. Zhen, C. Xu, J. Jiang, W. Shao, J. Tang, Synthesis, J. Magn. Magn. Mater. **323**, 515 (2011)
25. W. Lu, H. Yu, D. Sun, L. Lu, Part N J. Nanoeng. Nanosyst. **228**, 52 (2014)
26. S. Yan, L. Zhen, C. Xu, J. Jiang, W. Shao, J. Phys. D: Appl. Phys. **43**, 245003 (2010)
27. C. Wang, R. Lv, Z. Huang, F. Kang, J. Gu, J. Alloys Compd. **509**, 494 (2011)
28. N. Li, C. Hu, M. Cao, PCCP **15**, 7685 (2013)
29. F. Wen, F. Zhang, J. Xiang, W. Hu, S. Yuan, Z. Liu, J. Magn. Magn. Mater. **343**, 281 (2013)
30. C.K.L. Orhan, H. Montiel, G. Alvarez, M. Sharma, S. Pathak, M. Sharma, R. Singh, S. Saipriya, S. Widuch, *Ferromagnetic Resonance-Theory and Applications*. (InTech, Rijeka, Croatia, ISBN 978-953-51-1186-3, 2013)
31. J. Huo, L. Wang, H. Yu, J. Mater. Sci. **44**, 3917 (2009)
32. G.S. Wang, Y. Wu, Y.Z. Wei, X.J. Zhang, Y. Li, L.D. Li, B. Wen, P.G. Yin, L. Guo, M.S. Cao, Chem. Plus Chem. **79**, 375 (2014)
33. H. Kura, K. Hata, T. Oikawa, M. Takahashi, T. Ogawa, Scr. Mater. **76**, 65 (2014)
34. C.T. Fleaca, F. Dumitrache, I. Morjan, A.-M. Niculescu, I. Sandu, A. Ilie, I. Stamatin, A. Iordache, E. Vasile, G. Prodan, Appl. Surf. Sci. **374**, 213 (2016)
35. R. Alam, M. Mobin, J. Aslam, App. Surf. Sci. **368**, 360 (2016)

36. P. Zhang, X.U. Han, L.L. Kang, R. Qiang, W.W. Liu, Y.C. Du, RSC Adv. **3**, 12694 (2013)
37. S.H. Hosseini, P. Zamani, S.Y. Mousavi, J. Alloy Compd. **644**, 423 (2015)
38. S. Hosseini, P. Zamani, J. Magn. Magn. Mater. **397**, 205 (2016)
39. A. Tadjarodi, H. Kerdari, M. Imani, J. Alloy Compd. **554**, 284 (2013)
40. Z. He, Y. Fang, X. Wang, H. Pang, Synth. Met. **161**(8), 420 (2011)
41. J. Tang, L. Ma, N. Tian, M. Gan, F. Xu, J. Zeng, Mater. Sci. Eng. B **186**, 26 (2014)
42. F. Fievet, J.P. Lagier, B. Lin, B. Beaudoin, M. Figlarz, Solid State Ion. **32**, 198 (1989)
43. R.J. Joseyphus, T. Matsumoto, H. Takahashi, D. Kodama, K. Tohji, B. Jeyadevan, J. Solid State Chem. **180**(11), 3008 (2007)
44. R.J. Joseyphus, K. Shinoda, D. Kodama, B. Jeyadevan, Mater. Chem. Phys. **123**, 487 (2010)
45. P. Karipoth, A. Thirumurugan, R.J. Joseyphus, J. Colloid Interface Sci. **404**, 49 (2013)
46. R.S. Sundar, S.C. Deevi, Int. Mater. Rev. **50**, 157 (2005)
47. Z.J. Huba, K.J. Carroll, E.E. Carpenter, J. Appl. Phys. **109**, 07B514 (2011)
48. S.S.S. Afghahi, A. Shokuhfar, J. Magn. Magn. Mater. **370**, 37 (2014)